

A comparison of the gamma-ray bursts detected by BATSE and Swift[★]

D. Huja¹, A. Mészáros¹, and J. Řípa¹

Charles University, Faculty of Mathematics and Physics, Astronomical Institute, V Holešovičkách 2, 180 00 Prague 8, Czech Republic
e-mail: David.HUJA@seznam.cz, meszaros@cesnet.cz, ripa@sirrah.troja.mff.cuni.cz

Received 18 March 2008 / Accepted 22 May 2009

ABSTRACT

Aims. The durations of 388 gamma-ray bursts detected by the Swift satellite, are analyzed statistically to search for subgroups. The results are then compared with results obtained earlier for data from the BATSE database.

Methods. We apply the standard χ^2 test.

Results. As for data in the BATSE database, short and long subgroups are also reliably identified in the Swift data. An intermediate subgroup is also seen in the Swift database.

Conclusions. The analysis of the entire sample of 388 GRBs provides a support for the existence of three subgroups.

Key words. gamma rays: bursts

1. Introduction

During the years 1991–2000, 2704 gamma-ray bursts (GRBs) were detected by the BATSE instrument onboard the Compton Gamma-Ray Observatory (Meegan et al. 2001). After the launch of the Swift satellite (in November 2004), the frequency of GRBs detected by this instrument has been cca 100/year (Gehrels et al. 2005). Any comparison of different databases is highly useful. For example, in the BATSE database, three subgroups (short, intermediate, and long GRBs) have been robustly identified (Horváth et al. 2006; Chattopadhyay et al. 2007, and references therein). The short and long subgroups are physically different phenomena (Balázs et al. 2003). However, in contrast to this, it remains possible that the intermediate subgroup is not a true physically independent subgroup and it is present in the BATSE database because of e.g. some observational biases caused by the BATSE triggering procedure (Horváth et al. 2006). The most reliable way, to resolve the debate concerning whether subgroups or bias are present is to analyze an independent database acquired by another instrument. Hence, it is natural to ask whether these subgroups are also seen in the Swift data-set?

The purpose of this article is the statistical analysis of the Swift database, which may answer this question. We proceed in an identical way to the successful statistical analysis completed for the BATSE catalog (Horváth 1998) leading to the discovery of the third subgroup (Mukherjee et al. 1998; Bagoly et al. 1998; Horvath 1999; Hakkila et al. 2000; Rajaniemi & Mähönen 2002; Horváth 2002, 2003; Balázs et al. 2003; Horváth et al. 2006; Chattopadhyay et al. 2007). A statistical study of the Swift database – using the maximum likelihood method – has already shown evidence of a third subgroup (Horváth et al. 2008). The χ^2

fitting was not used because of the smallness of the population. However, historically, the first evidence of the third subgroup in the BATSE database came from the simple χ^2 method (Horváth 1998), and the number of 388 data points not should be too small for this testing. In all cases, one has to probe this fitting also for the Swift data sample. Since approximately one third of the Swift’s bursts have already well determined redshifts (in contrast to the BATSE’s GRBs, for which only a few objects have measured redshifts, Ramirez-Ruiz & Fenimore 2000; Norris 2002; Bagoly et al. 2003), some additional tests can also be done on samples with and without redshifts.

The paper is organized as follows. The samples are defined in Sect. 2 and also listed in detail at the end of the article. Section 3 presents the χ^2 fitting of these samples. Section 4 discusses the results of this paper, and Sect. 5 summarizes them.

2. The samples

We define two samples from the Swift data-set (Gehrels et al. 2005): the sample of GRBs without measured redshifts (z) and the sample with measured redshifts. These two samples are collected in Tables 4 and 5. We compiled these tables for convenience; each table contains the name of the GRB, its BAT duration T_{90} , and BAT fluence at range 15–150 keV, BAT 1-sec peak photon flux at range 15–150 keV, and Table 5 also provides its redshift. Only these bursts were taken into account, of which the GRB duration was measured. The combined data sets cover the period from November 2004 to the end of February 2009; the first (last) object is GRB041217 (GRB090205). Table 4 (5) contain 258 (130) GRBs, and hence the total number of GRBs, which are studied in this paper, is 388.

In this paper, we study both samples separately and also together as one single set (the complete sample).

[★] Tables 4 and 5 are only available in electronic form at <http://www.aanda.org>

Table 1. Results of the χ^2 fitting of the complete sample of 388 GRBs.

Fit	I.	II.	III.	IV.	V.	VI.	VII.
No. of bins	30	34	35	36	25	15	31
1 G							
χ_1^2	90.5	105.6	97.4	112.3	97.5	56.6	94.5
si. [%]	10^{-6}	10^{-8}	10^{-6}	10^{-8}	10^{-9}	10^{-5}	10^{-7}
μ	1.45	1.52	1.45	1.45	1.45	1.47	1.44
σ	0.87	0.88	0.89	0.87	0.93	0.83	0.89
2 G							
χ_2^2	30.9	40.1	31.3	47.7	17.3	7.5	23.1
si. [%]	15.6	6.5	34.4	2.1	58.8	58.6	57.1
μ_1	0.48	0.46	0.41	0.32	0.06	0.42	0.33
σ_1	0.93	0.99	0.98	0.95	1.09	0.92	0.97
μ_2	1.63	1.68	1.62	1.61	1.60	1.62	1.62
σ_2	0.51	0.52	0.52	0.53	0.54	0.53	0.52
w_2	0.84	0.76	0.85	0.88	0.85	0.83	0.82
F [%]	10^{-3}	10^{-4}	10^{-5}	10^{-4}	10^{-5}	10^{-2}	10^{-6}
3 G							
χ_3^2	21.4	29.7	22.6	35.9	10.0	2.4	16.7
si. [%]	43.6	23.7	65.5	11.6	86.7	88.2	78.0
μ_1	0.34	0.91	0.11	0.19	-0.01	1.07	0.28
σ_1	0.94	1.27	0.98	0.91	1.13	0.97	0.97
μ_2	1.19	1.18	1.24	1.04	1.06	1.12	1.62
σ_2	0.39	0.36	0.45	0.32	0.35	0.53	0.52
w_2	0.35	0.28	0.44	0.26	0.29	0.30	0.18
μ_3	1.91	1.93	1.94	1.84	1.85	1.84	1.84
σ_3	0.36	0.34	0.35	0.38	0.37	0.33	0.38
w_3	0.47	0.47	0.42	0.60	0.56	0.60	0.58
F [%]	4.04	4.66	3.07	4.50	2.52	3.63	5.41

3. χ^2 fitting of the GRB durations

3.1. The entire sample

Since the χ^2 fitting of the GRB duration distribution and the F-test were successfully used in the work Horváth (1998) (presenting the first evidence of three GRB subgroups), we proceed in an identical way, but with the Swift's data.

The complete sample consists of 388 events with measured T_{90} . We fitted the histogram of their decimal $\log T_{90}$ values seven times (fits I.–VII.). The results are collected in Table 1, and the fit No. VI. is seen in Fig. 1. We chose different binnings for independent fittings of various numbers of bins, with different bin edges. The bin widths also differ. In each bin, we applied the sole restriction that the theoretically expected number of GRBs should be higher than 5.

The histogram was first fitted with one single theoretical Gaussian curve of two free parameters (mean μ and standard deviation σ). The best-fit model parameters corresponding to the minimal χ^2 fit are, e.g., for fit No. VI the following: $\mu = 1.47$, $\sigma = 0.83$ with $\chi_1^2 = 56.6$. The goodness-of-fit for $15 - 2 - 1 = 12$ degrees of freedom (dof) provides a rejection at the level of $10^{-5}\%$ (Trumpler & Weaver 1953; Kendall & Stuart 1973). This represents a rejection of the null-hypothesis (i.e. one Gaussian curve is sufficient) that it is correct, because the probability of the mistake for this rejection is not higher than $10^{-5}\%$. The complete sample cannot be described by one single Gaussian curve. The same situation is also true for the remaining six fittings.

The fitting with the sum of two Gaussian curves (five free parameters: two means, two standard deviations, and one weight w_2 (since the first weight is equal to $1 - w_2$)) gave for the fit No. VI $\chi^2 = 7.5$. (Note that the value of w_2 requires that 17% (83%) of GRBs should belong to the short (long) subgroup.) Here d.o.f. = $15 - 5 - 1 = 9$ and we obtained an excellent fit with

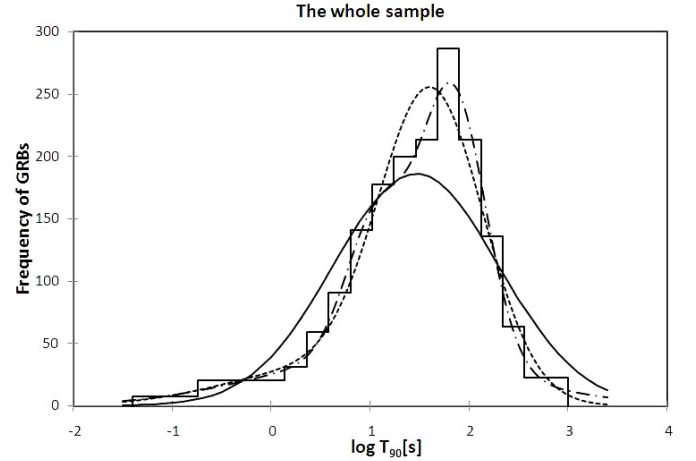


Fig. 1. Fitting of the $\log T_{90}$ histogram for the complete sample with 15 bins (fit No. VI.). The number of GRBs per bin is given by the product of the frequency and width. There are two equally populated bins between $-0.74 < \log T_{90} < 0.14$, divided at $\log T_{90} = -0.30$. For these bins, the frequencies are 20.45, and hence the number of GRBs in these bins equal to $20.45 \times 0.44 = 9$. The theoretical curves show the best fits: full line = 1 Gaussian curve; dotted line = sum of 2 Gaussian curves; dash-dotted line = sum of 3 Gaussian curves.

the significance level 58.6% (i.e., if we suppose that the fit is incorrect, then the probability that this assumption is wrong is higher than 58.6%). The assumption that the duration distribution is represented by the sum of two Gaussian curves cannot be – from the statistical point of view – rejected. The best-fit curve is also presented in Fig. 1, showing a good correspondence with measured data. The remaining six fits again provide similar results.

We also performed the fitting with the sum of three Gaussian curves (eight parameters: three means, three standard deviations, and two independent weights), and obtained an excellent fit with $\chi_3^2 = 2.4$ for fit no. VI, because the goodness-of-fit implies that for d.o.f. = $15 - 8 - 1 = 6$, the significance level is 88.2%. The best-fit curve is also seen in Fig. 1, which indicates closer correspondence with the measured data. The same excellent fits are also obtained for the remaining six binnings.

The key question is whether the decreasing $\Delta\chi^2 = 7.5 - 2.4 = 5.1$ is statistically significant? To answer this question, we proceed similarly to Horváth (1998) and used the test proposed by Band et al. (1997) in Appendix A. The significance level from the F-test is 3.63%. This implies that the rejection of the null-hypothesis (i.e. that the sum of the two Gaussian curves is enough) is adequate, because the probability of the mistake at this rejection level is not higher than 3.63%. We arrive at the conclusion that the strengthening of χ^2 need not be a fluctuation. Similar results were obtained for the remaining six fits – only for fit No. VII was the significance just above the usual 5% limit. (The significances lower than 5% are denoted by boldface.) In other words, the introduction of the third subgroup – purely from the statistical point of view – is significant for six of the seven fits completed. We note that the same F-test can also be applied to the difference $\chi_1^2 - \chi_2^2$, and we always obtain the conclusion that the introduction of the second subgroup – instead of the one single group – is strongly supported.

3.2. The sample with z

The sample contains 130 events with duration information. We also performed seven fits, but the number of bins had to be

Table 2. Results of the χ^2 fitting of the sample of 130 GRBs with the known redshifts.

Fit	I.	II.	III.	IV.	V.	VI.	VII.
No. of bins	10	11	12	15	16	17a	17b
1 G							
χ^2_1	9.7	12.2	13.9	11.8	14.8	16.8	11.9
si.[%]	20.9	14.4	12.6	46.0	31.8	26.5	61.2
μ	1.55	1.52	1.53	1.69	1.54	1.54	1.53
σ	0.74	0.77	0.74	0.78	0.76	0.75	0.76
2 G							
χ^2_2	2.6	6.7	7.7	4.7	7.9	10.1	5.3
si.[%]	62.4	24.0	26.0	86.0	64.0	51.8	91.8
μ_1	1.47	-0.50	0.17	0.22	0.70	-0.69	-0.66
σ_1	0.77	1.00	0.88	0.94	0.86	0.10	0.15
μ_2	1.97	1.58	1.62	1.77	1.68	1.59	1.58
σ_2	0.10	0.63	0.58	0.60	0.55	0.62	0.63
w_2	0.12	0.97	0.91	0.91	0.82	0.97	0.97
F[%]	6.97	28.21	22.19	2.20	6.50	9.74	1.70
3 G							
χ^2_3	2.0	2.0	1.9	2.2	4.0	5.4	2.8
si.[%]	15.4	49.8	59.1	89.9	77.8	71.4	94.8
μ_1	1.04	-0.13	1.16	0.17	1.07	-0.57	-0.12
σ_1	0.30	1.00	1.05	0.50	0.92	0.05	0.14
μ_2	1.17	0.94	1.61	1.14	1.32	1.12	0.95
σ_2	1.10	0.26	0.25	0.26	0.12	0.42	0.33
w_2	0.25	0.24	0.53	0.24	0.49	0.48	0.28
μ_3	1.94	1.85	1.91	2.00	1.88	2.00	1.86
σ_3	0.34	0.44	0.18	0.43	0.33	0.34	0.43
w_3	0.49	0.69	0.25	0.67	0.41	0.49	0.67
F[%]	89.64	24.41	10.51	13.29	12.66	11.40	10.96

reduced because of the lower number of objects in the sample. We again in a different way binned data – fits VI. and VII. had 17 bins, but the structure was different. In each bin again the number of GRBs was higher than 5. The results are collected in Table 2, and fit No.II. is shown in Fig. 2.

Here the results, compared with the entire sample, differ for two reasons. First, the fits with one single Gaussian curve are also acceptable, and only for two fits does the F-test show that the introduction of the second subgroup is adequate. Second, the introduction of the third subgroup is not needed from the F-test. All this indicates that this sample can be defined by one single group, and even the separation between short and long GRBs is not needed.

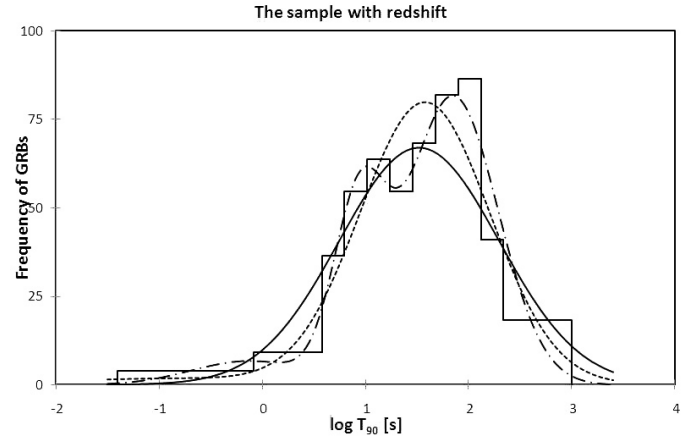
3.3. The sample without z

This sample contains 258 events with duration information. We also completed seven fits with different binnings. In each bin, the number of GRBs was again higher than 5. The results are presented in Table 3, and fit No.I. is shown in Fig. 3.

Compared with the entire sample, the results are similar – except that, the introduction of the third subgroup is not needed according to the F-test. All of this shows that this sample can be described well by the sum of two and only two subgroups.

4. Discussion of the results

We first highlight that we have proven that short and long subgroups also exist in the Swift data-set. Both the complete sample and the sample with no redshifts have been found to contain these two subgroups, because fits attempted with one single Gaussian curve are clearly wrong. It is also remarkable that

**Fig. 2.** Fitting of $\log T_{90}$ in the sample with known redshifts. The theoretical curves show the best-fit curves. The notation of the lines is the same as in Fig. 1.**Table 3.** Results of the χ^2 fitting of the sample without the known redshift with 258 GRBs.

Fit	I.	II.	III.	IV.	V.	VI.	VII.
No. of bins	11	14	16	18	20	22	23
1 G							
χ^2_1	57.8	66.8	67.3	71.4	76.0	83.8	76.2
si.[%]	10^{-7}	10^{-8}	10^{-7}	10^{-7}	10^{-7}	10^{-8}	10^{-6}
μ	1.47	1.41	1.41	1.41	1.41	1.42	1.41
σ	0.83	0.90	0.86	0.90	0.87	0.90	0.88
2 G							
χ^2_2	6.9	9.5	15.1	13.7	18.2	23.2	19.5
si.[%]	22.8	30.6	13.0	31.8	20.0	10.9	30.0
μ_1	-0.04	0.09	0.36	0.22	0.38	0.28	0.48
σ_1	0.81	1.07	0.98	1.06	1.00	1.03	1.03
μ_2	1.58	1.60	1.60	1.61	1.62	1.62	1.63
σ_2	0.51	0.51	0.49	0.50	0.48	0.49	0.48
w_2	0.86	0.83	0.80	0.81	0.79	0.80	0.76
F[%]	0.36	0.04	0.07	0.01	0.01	0.01	10^{-3}
3 G							
χ^2_3	2.9	3.1	10.6	9.2	14.8	18.3	17.0
si.[%]	23.3	68.2	15.8	42.1	19.1	14.5	25.9
μ_1	-0.46	-0.55	-0.52	-0.38	0.97	-0.38	-0.12
σ_1	0.40	0.82	0.59	0.80	1.13	0.78	0.86
μ_2	0.86	1.47	1.37	1.51	1.15	1.48	1.52
σ_2	0.33	0.56	0.57	0.57	0.19	0.56	0.55
w_2	0.20	0.77	0.67	0.78	0.17	0.74	0.74
μ_3	1.72	1.97	1.89	1.91	1.82	1.94	1.88
σ_3	0.43	0.15	0.28	0.15	0.29	0.20	0.20
w_3	0.72	0.13	0.25	0.11	0.45	0.15	0.13
F[%]	40.20	6.81	39.50	23.87	47.00	33.60	53.60

the weight of the short subgroup agrees with this expectation. As follows from Horváth et al. (2006), in the BATSE catalog the populations of the short, intermediate, and long bursts are have in terms of number the ratio 20:10:70. Nevertheless, because the short bursts are harder and Swift is more sensitive to softer GRBs, one may expect that in the Swift database the population of short GRBs should be comparable to or lower than 20% because of instrumental reasons. The weights derived for the entire sample (being between 10 and 26%) agree with this expectation. Entire the other values of the best-fit model parameters – i.e. two means and two standard deviations – are also roughly in

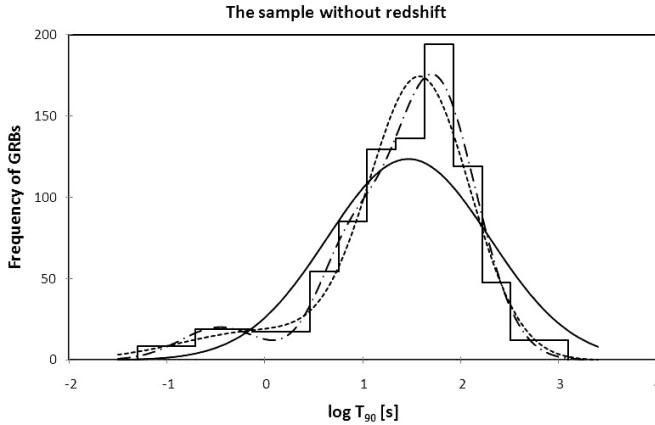


Fig. 3. Fitting of $\log T_{90}$ to the sample with unknown redshifts. The theoretical curves show the best fits. The notation of the lines is the same as in Fig. 1.

the ranges expected on the basis of the BATSE values. The differences can be given by the different instrumentations. For example, the mean values of the $\log T_{90}$ should be slightly longer in the Swift database than for the BATSE data (Barthelmy et al. 2005; Band 2006). In Horváth (1998), the BATSE's means are -0.35 (short) and 1.52 (long), respectively. We obtained for the complete sample values from -0.01 to 0.91 (short) and from 1.60 to 1.94 (long), respectively. In terms of short and long GRBs, all this implies that the situation is almost identical to that of the BATSE data-set.

For the sample with known redshifts, the situation is different, because the fits still allow one single Gaussian curve. This result can be easily explained by selection effects. It is well-known that the observational determination of the redshifts in the Swift data sample is easier for long than short bursts because of observational strategies, i.e., it is more complicated to detect and follow the afterglows of short GRBs (Gehrels et al. 2005).

Concerning the third intermediate subgroup, the complete sample also supports its existence six out of seven tests inferred significances of below 5%. Hence, strictly speaking, the third subclass does exist and the probability of the mistake in this claim is not higher than $x\%$, where $2.52 < x < 5.41$. This result agrees with expectations, once a comparison with the BATSE database is provided. As stated in the Introduction, for the BATSE database the first evidence of a third subgroup was provided by this χ^2 method, and hence for the Swift database this test should also provide positive support for this subgroup, if the two datasets are comparable. It is the key result of this article that this expectation is fulfilled. Our study has shown that the classical χ^2 fitting – in combination with F-test – may well also work in the Swift database as for the BATSE database (Horváth 1998).

Horváth et al. (2008) confirmed the existence of a third subgroup in the Swift dataset by applying the maximum likelihood (ML) method. Our significance of between 2.52% and 5.41% is weaker than the 0.46% significance obtained by Horváth et al. (2008), as expected, because the ML method is a more robust statistical test. This is seen from new two studies, too: the ML test applied to the databases of RHESSI (Řípa et al. 2009) and BeppoSAX (Horváth 2009) satellites, respectively, confirmed the existence of the third intermediate subclass; on the other hand, the χ^2 test was either not of high enough significance

for RHESSI data (Řípa et al. 2009) or was not used at all for BeppoSAX data (Horváth 2009).

It is also expected that the mean $\log T_{90}$ for the intermediate group should be much higher in the Swift database because of the different redshift distributions (Band 2006; Jakobsson et al. 2006; Bagoly et al. 2006). The mean value of the BATSE's intermediate subgroup is 0.64 (Horváth 1998), but here the value is between 1.02 and 1.64. Horváth et al. (2008) also obtained a similar value of (1.107). Hence, the typical durations also agree with expectations.

The sample with no redshifts exhibited to sign of a third subgroup, which may be due to the lower number of objects in the sample. The sample with known redshifts is strongly biased by selection effects, and even here the existence of the short subgroup was unclear. Hence, we conclude that the existence of a third subgroup is unclear.

5. Conclusions

Since the χ^2 fitting of the GRB duration distribution and the F-test were successfully used in the work Horváth (1998), which presented the first evidence of three GRB subgroups, we have proceeded identically, but with the Swift's data.

The results may be summarized in the following four points:

1. For the short and long subgroups, all of our findings agree with expectations: they are also detected in the Swift database and weight of the short subgroup is lower, which may be because of the Swift's higher effective sensitivity to softer bursts.
2. The complete sample of 388 objects appears to contain three subgroups, because from seven fits the complete sample, six have confirmed the existence of the intermediate subgroup on a lower than 5% significance level. Hence, for the Swift database, the situation is similar to that of the BATSE dataset, although our significances are lower than the measurement of $>0.02\%$ of Horváth (1998).
3. The samples with and without known redshifts are separately either not enough populated, or strongly biased. Hence, no far reaching conclusions can be drawn about them.
4. As for the BATSE database, it is shown again that the classical χ^2 test – in combination with the F-test – is also effective for the Swift GRB sample.

Acknowledgements. Thanks are due to valuable discussions with Z. Bagoly, L.G. Balázs, I. Horváth, and P. Veres. This study was supported by the GAUK grant No. 46307, by the OTKA grants No. T48870 and K77795, by the Grant Agency of the Czech Republic grant No. 205/08/H005, and by the Research Program MSM0021620860 of the Ministry of Education of the Czech Republic. The useful remarks of the referee, C. Guidorzi, are kindly acknowledged.

References

- Bagoly, Z., Csabai, I., Mészáros, A., et al. 2003, A&A, 398, 919
 Bagoly, Z., Mészáros, A., Balázs, L. G., et al. 2006, A&A, 453, 797
 Bagoly, Z., Meszaros, A., Horvath, I., Balazs, L. G., & Meszaros, P. 1998, ApJ, 498, 342
 Balázs, L. G., Bagoly, Z., Horváth, I., Mészáros, A., & Mészáros, P. 2003, A&A, 401, 129
 Band, D. L. 2006, ApJ, 644, 378
 Band, D. L., Ford, L. A., Matteson, J. L., et al. 1997, ApJ, 485, 747
 Barthelmy, S. D., Chincarini, G., Burrows, D. N., et al. 2005, Nature, 438, 994

- Chattopadhyay, T., Misra, R., Chattopadhyay, A. K., & Naskar, M. 2007, *ApJ*, 667, 1017
- Gehrels et al. 2005, (Swift team),
http://heasarc.gsfc.nasa.gov/docs/swift/archive/grb_table/
- Hakkila, J., Haglin, D. J., Pendleton, G. N., et al. 2000, *ApJ*, 538, 165
- Horváth, I. 1998, *ApJ*, 508, 757
- Horvath, I. 1999, *J. Korean Phys. Soc.*, 35, 629
- Horváth, I. 2002, *A&A*, 392, 791
- Horváth, I. 2003, *Statistical Challenges in Modern Astronomy III.*, ed. E. D. Feigelson & G. J. Babu (Berlin: Springer), 439
- Horváth, I. 2009, *ASS*, in press, [arXiv:0905.0860]
- Horváth, I., Balázs, L. G., Bagoly, Z., Ryde, F., & Mészáros, A. 2006, *A&A*, 447, 23
- Horváth, I., Balázs, L. G., Bagoly, Z., & Veres, P. 2008, *A&A*, 489, L1
- Jakobsson, P., Levan, A., Fynbo, J. P. U., et al. 2006, *A&A*, 447, 897
- Kendall, M. G. & Stuart, A. 1973, *The Advanced Theory of Statistics* (London: Griffin)
- Meegan, C. A., et al. 2001, *Current BATSE Gamma-Ray Burst Catalog*,
<http://gammaray.msfc.nasa.gov/batse/grb/catalog>
- Mukherjee, S., Feigelson, E. D., Jogesh Babu, G., et al. 1998, *ApJ*, 508, 314
- Norris, J. P. 2002, *ApJ*, 579, 386
- Rajaniemi, H. J. & Mähönen, P. 2002, *ApJ*, 566, 202
- Ramirez-Ruiz, E. & Fenimore, E. E. 2000, *ApJ*, 539, 712
- Trumpler, R. J. & Weaver, H. F. 1953, *Statistical Astronomy* (Berkeley: University of California Press)
- Řípa, J., Mészáros, A., Wigger, C., et al. 2009, *A&A*, 498, 399

Table 4. Swift GRBs with no measured redshifts; Part I.

GRB	T_{90} s	fluence 10^{-7} erg/cm ²	peak-flux ph/(cm ² s)
090201	83.0	300.00	14.70
090129	17.5	21.00	3.70
090123	131.0	29.00	1.70
090118	16.0	4.00	n/a
090113	9.1	7.60	2.50
090111	24.8	6.20	0.90
090107A	12.2	2.30	1.10
081230	60.7	8.20	0.70
081228	3.0	0.89	0.60
081226A	0.4	0.99	2.40
081221	34.0	181.00	18.20
081211A	3.5	1.30	0.80
081210	146.0	18.00	2.50
081203B	23.4	21.00	n/a
081128	100.0	23.00	1.30
081127	37.0	4.90	0.60
081126	54.0	33.00	3.70
081109A	190.0	36.00	1.10
081104	59.1	20.00	1.00
081102	63.0	23.00	1.40
081101	0.2	0.62	3.60
081025	23.0	19.00	1.30
081024A	1.8	1.20	1.10
081022	160.0	25.00	0.60
081017	320.0	14.00	0.07
081016B	2.6	0.99	0.50
081012	29.0	11.00	1.00
081011	9.0	1.60	0.40
080919	0.6	0.72	1.20
080916B	32.0	6.30	0.60
080915B	3.9	9.90	8.50
080915A	14.0	2.30	0.50
080905A	1.0	1.40	1.30
080903	66.0	14.00	0.80
080822B	64.0	1.70	0.06
080802	176.0	13.00	0.30
080727C	79.7	52.00	2.30
080727B	8.6	31.00	7.60
080727A	4.9	1.30	0.30
080725	120.0	37.00	2.30
080723A	17.3	3.30	0.90
080714	33.0	25.00	4.20
080703	3.4	2.00	1.00
080702B	20.0	5.00	0.50
080702A	0.5	0.36	0.70
080701	18.0	7.10	2.20

Table 4. Swift GRBs with no measured redshifts; Part II.

GRB	T_{90} s	fluence 10^{-7} erg/cm ²	peak-flux ph/(cm ² s)
080623	15.2	10.00	2.00
080613B	105.0	58.00	2.70
080602	74.0	32.00	2.90
080524	9.0	2.90	0.40
080523	102.0	8.80	0.50
080517	64.6	5.60	0.60
080515	21.0	20.00	3.90
080506	150.0	13.00	0.40
080503	170.0	20.00	0.90
080426	1.7	3.70	4.80
080409	20.2	6.10	3.70
080405	40.0	12.00	n/a
080328	90.6	94.00	5.50
080325	128.4	49.00	1.40
080320	14.0	2.70	0.60
080319D	24.0	3.20	0.10
080319A	64.0	48.00	1.20
080315	65.0	1.40	0.04
080307	125.9	8.70	0.40
080303	67.0	6.60	1.40
080229A	64.0	90.00	5.70
080218B	6.2	5.10	3.10
080218A	27.6	6.30	1.40
080212	123.0	29.00	1.20
080207	340.0	61.00	1.00
080205	106.5	21.00	1.40
080130	65.0	7.70	0.20
080129	48.0	8.90	0.20
080123	115.0	5.70	1.80
080121	0.7	0.30	n/a
071129	420.0	35.00	0.90
071118	71.0	5.00	0.30
071112B	0.3	0.48	1.30
071110	19.0	0.76	0.40
071028B	55.0	2.50	1.40
071028A	27.0	3.00	0.30
071025	109.0	65.00	1.60
071018	376.0	10.00	0.20
071013	26.0	3.20	0.40
071011	61.0	22.00	1.70
071008	18.0	2.40	0.50
071006	50.0	1.40	13.00
071001	58.5	7.70	0.90
070923	0.1	0.10	2.40
070920B	20.2	6.60	0.80
070920A	56.0	5.10	0.30
070917	7.3	20.00	8.50
070913	3.2	2.50	1.40
070911	162.0	120.00	3.90

Table 4. Swift GRBs with no measured redshifts; Part III.

GRB	T_{90} s	fluence 10^{-7} erg/cm ²	peak-flux ph/(cm ² s)
070810B	80.0	0.12	1.80
070809	1.3	1.00	1.20
070808	32.0	12.00	2.00
070805	31.0	7.20	0.70
070731	2.9	1.60	1.20
070729	0.9	1.00	1.00
070721A	3.4	0.71	0.70
070714A	2.0	1.50	1.80
070704	380.0	59.00	2.10
070628	39.1	35.00	5.10
070621	33.3	43.00	2.50
070616	402.0	192.00	1.90
070612B	13.5	17.00	2.60
070610	4.6	2.40	0.90
070531	44.0	11.00	1.00
070520B	66.0	9.20	0.40
070520A	18.0	2.50	0.40
070518	5.5	1.60	0.70
070517	9.0	2.60	0.80
070509	7.7	1.70	0.70
070429B	0.5	0.63	1.80
070429A	163.0	9.20	0.40
070427	11.0	7.20	1.30
070420	77.0	140.00	7.10
070419B	236.5	75.00	1.40
070412	34.0	4.80	0.70
070406	0.7	0.45	0.70
070330	9.0	1.80	0.90
070328	69.0	89.00	4.20
070227	7.0	16.00	2.70
070224	34.0	3.10	0.30
070223	89.0	17.00	0.70
070220	129.0	106.00	5.88
070219	17.0	3.20	0.70
070209	0.1	0.11	2.40
070129	460.0	31.00	0.60
070126	51.0	1.60	0.20
070103	19.0	3.40	1.10
061222A	72.0	83.00	9.20
061218	4.1	0.20	0.41
061202	91.0	35.00	2.60
061126	191.0	72.00	9.80
061102	17.6	1.90	0.20
061028	106.0	9.70	0.70
061027	150.0	4.70	0.08
061021	46.0	30.00	6.10
061019	191.0	17.00	2.20
061006	130.0	14.30	5.36
061004	6.2	5.70	2.50
061002	17.6	6.80	0.80
060929	12.4	2.80	0.40
060923C	76.0	16.00	1.00
060923B	8.8	4.80	1.50
060923A	51.7	8.70	1.30
060919	9.1	5.50	2.20
060904A	80.0	79.00	4.90

Table 4. Swift GRBs with no measured redshifts; Part IV.

GRB	T_{90} s	fluence 10^{-7} erg/cm ²	peak-flux ph/(cm ² s)
060825	8.1	9.80	2.70
060813	14.9	55.00	9.00
060807	34.0	7.30	0.80
060805	5.4	0.74	0.30
060804	16.0	5.10	1.20
060801	0.5	0.81	1.30
060728	60.0	2.40	n/a
060719	55.0	16.00	2.30
060717	3.0	0.65	0.50
060712	26.0	13.00	1.70
060607B	31.0	17.00	1.50
060602A	60.0	16.00	0.50
060516	160.0	11.00	0.30
060515	52.0	14.00	0.80
060510A	21.0	98.00	17.00
060507	185.0	45.00	1.30
060501	26.0	12.00	1.90
060428B	58.0	7.20	0.60
060428A	39.4	14.00	2.40
060427	64.0	5.00	0.30
060424	37.0	6.80	1.60
060421	11.0	12.00	3.00
060413 1	50.0	36.00	0.90
060403	30.0	14.00	1.00
060323	18.0	5.70	0.80
060322	213.0	51.00	2.10
060319	12.0	2.70	1.10
060313	0.7	11.30	12.10
060312	43.0	18.00	1.50
060306	61.0	22.00	6.10
060223B	10.2	16.00	2.90
060219	62.0	4.20	0.60
060211B	29.0	4.70	0.70
060211A	126.0	15.00	0.40
060204B	134.0	30.00	1.30
060203	60.0	8.50	0.60
060202	203.7	24.00	0.50
060117	16.0	204.00	48.90
060111B	59.0	16.00	1.40
060111A	13.0	11.80	1.72
060110	17.0	14.00	1.90
060109	116.0	6.40	0.50
060105	55.0	182.00	7.50
060102	21.0	2.40	0.40
051227	8.0	2.30	0.97
051221B	61.0	11.30	0.54
051213	70.0	8.00	0.51
051210	1.4	0.83	0.75
051117B	8.0	1.40	0.46
051117A	140.0	46.00	0.93
051114	2.2	1.32	0.73
051113	94.0	26.00	2.40
051105A	0.3	0.20	2.00
051021B	47.0	9.10	0.63
051016A	22.0	8.80	1.60
051012	13.0	2.90	0.60
051008	16.0	58.00	5.50
051006	26.0	12.80	1.90
051001	190.0	18.00	0.51

Table 4. Swift GRBs with no measured redshifts; Part V.

GRB	T_{90} s	fluence 10^{-7} erg/cm ²	peak-flux ph/(cm ² s)
050925	0.1	0.75	1.50
050922B	250.0	26.00	1.02
050916	90.0	11.00	0.69
050915B	40.0	34.00	2.34
050915A	53.0	8.80	0.80
050911	16.0	3.01	1.31
050906	0.1	0.07	1.15
050827	49.0	21.20	1.86
050822	102.0	26.10	2.47
050820B	13.0	21.20	4.06
050819	36.0	3.52	0.39
050815	2.8	0.92	0.56
050801	20.0	3.12	1.47
050721	39.0	30.80	3.08
050717	86.0	61.70	6.34
050715	52.0	14.40	1.07
050713A	70.0	52.50	4.78
050712	48.0	11.00	0.55
050701	22.0	13.60	2.77
050607	26.5	6.05	0.99
050528	10.8	4.40	1.23
050509A	11.6	3.38	0.88
050502B	17.5	4.72	1.43
050422	59.2	6.15	0.57
050421	10.3	1.18	0.44
050418	83.0	53.90	3.80
050416B	5.4	11.30	5.85
050412	26.0	5.66	0.49
050410	43.0	43.00	1.80
050326	29.5	90.50	12.40
050306	160.0	120.00	3.64
050219B	27.0	164.00	25.40
050219A	23.0	42.10	3.61
050215B	8.0	2.33	0.68
050215A	6.0	7.29	0.51
050202	0.1	0.33	2.98
050128	13.8	51.70	7.59
050124	4.1	12.30	5.57
050117	169.0	91.20	2.40
041228	62.0	36.10	1.65
041226	15.0	3.23	0.34
041224	235.0	75.30	2.95
041223	107.0	171.00	7.49
041220	5.0	3.82	1.83
041219C	40.0	20.00	1.50
041219B	30.0	n/a	10.00
041219A	520.0	1000.00	25.00
041217	7.5	65.70	4.40

Table 5. Swift GRBs with known redshifts; Part I.

GRB	T_{90} s	fluence 10^{-7} erg/cm ²	peak-flux ph/(cm ² s)	z
090205	8.8	1.90	0.50	4.6749
090102	27.0	0.68	5.50	1.5477
081222	24.0	48.00	7.70	2.7467
081203A	294.0	77.00	2.90	2.1000
081121	14.0	41.00	4.40	2.5120
081118	67.0	12.00	0.60	2.5800
081029	270.0	21.00	0.50	3.8474
081028A	260.0	37.00	0.50	3.03800
081008	185.5	43.00	1.30	1.96775
081007	10.0	7.10	2.60	0.52950
080928	280.0	25.00	2.10	1.6910
080916A	60.0	40.00	2.70	0.68900
080913	8.0	5.60	1.40	6.57000
080906	147.0	35.00	1.00	2.00000
080905B	128.0	18.00	0.50	2.37400
080810	106.0	46.00	2.00	3.35000
080805	78.0	25.00	1.10	1.50500
080804	34.0	36.00	3.10	2.20225
080721	16.2	120.00	20.90	2.59650
080710	120.0	14.00	1.00	0.84500
080707	27.1	5.20	1.00	1.23000
080607	79.0	240.00	23.10	3.03600
080605	20.0	133.00	19.90	1.63980
080604	82.0	8.00	0.40	1.41600
080603B	60.0	24.00	3.50	2.69000
080520	2.8	0.55	0.50	1.54500
080516	5.8	2.60	1.80	3.20000
080430	16.2	12.00	2.60	0.75850
080413B	8.0	32.00	18.70	1.10000
080413A	46.0	35.00	5.60	2.43300
080411	56.0	264.00	43.20	1.03000
080330	61.0	3.40	0.90	1.51000
080319C	34.0	36.00	5.20	1.95000
080319B	50.0	810.00	24.80	0.93700
080310	365.0	23.00	1.30	2.42580
080210	45.0	18.00	1.60	2.64100

Table 5. Swift GRBs with known redshifts; Part II.

GRB	T_{90} s	fluence 10^{-7} erg/cm ²	peak-flux ph/(cm ² s)	z
071227	1.8	2.20	1.60	0.3835
071122	68.7	5.80	0.40	1.14
071117	6.6	24.00	11.30	1.331
071112C	15.0	30.00	8.00	0.82
071031	180.0	9.00	0.50	2.692
071021	225.0	13.00	0.70	5.0
071020	4.2	23.00	8.40	2.1435
071010B	35.7	44.00	7.70	0.947
071010A	6.0	2.00	0.80	0.98
071003	150.0	83.00	6.30	1.0185
070810A	11.0	6.90	1.90	2.17
070802	16.4	2.80	0.40	2.45
070724A	0.4	0.80	1.00	0.457
070721B	340.0	36.00	1.50	3.626
070714B	64.0	7.20	2.70	0.92
070612A	370.0	110.00	1.50	0.617
070611	12.0	39.00	0.80	2.04
070529	109.0	26.00	1.40	2.4996
070521	37.9	80.00	6.70	0.553
070508	21.0	200.00	24.70	0.82
070506	4.3	2.10	1.00	2.31
070419A	116.0	5.60	2.80	0.97
070411	101.0	25.00	1.00	2.954
070318	63.0	23.00	1.60	0.838
070306	210.0	55.00	4.20	1.497
070208	48.0	4.30	0.90	1.165
070110	85.0	16.00	0.60	2.352
061222B	40.0	22.00	1.50	3.355
061217	0.3	0.46	1.30	0.827
061210	85.0	11.00	5.30	0.41
061201	0.8	3.30	3.90	0.111
061121	81.0	137.00	21.10	1.314
061110B	128.0	13.00	0.40	3.44
061110A	41.0	11.00	0.50	0.758
061007	75.0	450.00	15.30	1.2615
060927	22.6	11.00	2.80	5.6
060926	8.0	2.20	1.10	3.208
060912	5.0	13.00	8.50	0.937
060908	19.3	29.00	3.20	2.43
060906	43.6	22.10	2.00	3.685
060904B	192.0	17.00	2.50	0.703
060814	146.0	150.00	7.40	0.84
060729	116.0	27.00	1.40	0.54
060714	115.0	30.00	1.40	2.71
060708	9.8	5.00	2.00	2.3
060707	68.0	17.00	1.10	3.43

Table 5. Swift GRBs with known redshifts; Part III.

GRB	T_{90} s	fluence 10^{-7} erg/cm ²	peak-flux ph/(cm ² s)	z
060614	102.0	217.00	11.60	0.1275
060607A	100.0	26.00	1.40	3.082
060605	15.0	4.60	0.50	3.76
060604	10.0	1.30	0.60	2.68
060526	13.8	4.90	1.70	3.21
060522	69.0	11.00	0.60	5.11
060512	8.6	2.30	0.90	0.4428
060510B	276.0	42.00	0.60	4.9
060505	4.0	6.20	1.90	0.089
060502B	90.0	0.40	4.40	0.287
060502A	33.0	22.00	1.70	1.51
060418	52.0	81.00	6.70	1.4895
060223A	11.0	6.80	1.40	4.41
060210	255.0	77.00	2.80	3.91
060206	7.0	8.40	2.80	4.048
060123	900.0	3.00	0.04	1.099
060116	113.0	26.00	1.10	5.3
060115	142.0	18.00	0.90	3.53
060108	14.4	3.70	0.70	2.03
051221A	1.4	11.60	12.10	0.547
051111	47.0	39.00	2.50	1.549
051109B	15.0	2.70	0.50	0.08
051109A	36.0	21.00	3.70	2.346
051016B	4.0	1.70	1.32	0.9364
050922C	5.0	17.00	7.36	2.198
050908	20.0	4.91	0.70	3.3459
050904	225.0	50.70	0.66	6.29
050826	35.0	4.51	0.43	0.297
050824	25.0	2.92	0.52	0.83
050820A	26.0	40.10	2.50	2.61335
050814	65.0	18.30	0.75	5.3
050813	0.6	0.43	0.92	1.80
050803	85.0	22.30	1.08	0.422
050802	13.0	22.00	2.65	1.71
050730	155.0	24.20	0.57	3.9669
050724	3.0	11.80	3.29	0.2575
050603	13.0	76.30	27.60	2.821
050525A	8.8	156.00	42.30	0.606
050509B	0.04	0.13	1.33	0.225
050505	60.0	24.90	1.81	4.27
050416A	2.4	4.31	4.97	0.6535
050406	3.0	0.81	0.38	2.44
050401	33.0	85.50	12.60	2.9
050319	10.0	6.25	1.45	3.24
050318	32.0	13.10	3.20	1.44
050315	96.0	32.30	1.98	1.949
050223	23.0	6.40	0.70	0.58775
050126	26.0	8.60	0.70	1.29